THEORETICAL & APPLIED MECHANICS LETTERS **3**, 042001 (2013)

A review on research of fire dynamics in high-rise buildings

Jinhua Sun,[a] Longhua Hu,[b] and Ying Zhang
State Key Laboratory of Fire Science, University of Science and Technology of China, Hefei 230026, China

(Received 20 May 2013; accepted 22 June 2013; published online 10 July 2013)

Abstract Since serious fire occurred frequently in recent years, fire safety of high-rise building has attracted extensive attention. A National Basic Research Program (973 program) of China has been set up by Ministry of Science and Technology (MOST) of China in 2012 to meet the research requirements of fire safety in high-rise buildings. This paper reviews the current state of art of research on fire dynamics of high-rise buildings, including the up-to-date progress of this project. The following three subjects on fire dynamics of high-rise buildings are addressed in this review: the ejected flame and fire plume behavior over facade out of the compartment window, the flame spread behavior over facade thermal insulation materials, and the buoyancy-driven smoke transportation characteristics along long vertical channels in high-rise buildings. Prospective future works are discussed and summarized. [doi:10.1063/2.1304201]

Keywords high-rise building, fire dynamics, facade flame, fire spread, smoke transportation

I. INTRODUCTION

With China's social and economic development and urbanization, the number of (ultra-) high-rise buildings is increasing at an unexpected speed. In China, almost 1.5% high-rise buildings are ultra-high-rise ones. However, these high-rise buildings bring serious fire risks. Due to the weakness of fire prevention capability in high-rise buildings, once a fire begins, human life, animal life, health, or property are all threatened.

Several large fires which attracted great attention all occurred in high-rise buildings. In 2009, a massive blaze happened in the uncompleted Television Cultural Center (TVCC) in Beijing caused one firefighter's death, seven injuries and more than 4 billion yuan in damages. The 2010 Shanghai fire destroyed a 28-story high-rise building, killed at least 58 people, and injured over 70 others. In addition, the Harbin Jingwei 360 degree Building fire in 2008, the Shenyang Royal Wanxin Building fire in 2011, and the World Trade Center fire in New York in 2001 all resulted in great damages. In a word, high-rise fire could result in terrible casualties and serious damages. This issue becomes one of the most concerned topic in public and calls for researches in this field eagerly.

Compared to normal room fires, the fire behaviors in high-rise buildings have some new special features.

(1) The extensive use of the external facade insulation materials brings new fire safety issues. Due to the demand for energy-saving, wall insulation materials are widely used in high-rise buildings. The exterior organic insulation materials, such as polystyrene and polyurethane, are of superior energy-saving insulation performance. However, once these combustible insulation materials ignited, flame spreads very fast over their surface, and produce large amount of toxic products. Fire safety issues of external facade insulation materials have become a major problem for high-rise building.

(2) Complex building structures and boundary environment could also lead to special fire evolution behavior. Once the high-rise building with complex structure catches a fire, stairwells, elevator shafts and tube wells in the building can cause stack effect, piston effect, etc. This will significantly contribute to the spread of fire and smoke transport processes. Furthermore, if the indoor fire lead to the rupture of the glass curtain wall and come out of the window, the fire will not be easily controlled at all. Existing building fire dynamics model can not explain and predict this kind of high-rise fire phenomena and behavior.

(3) Fire also brings threats to the structures of high-rise buildings. Major structures such as glass walls and steel structures lead to very complex mechanical load distribution. The key components and nodes in the structure system are very likely to fail or even collapse due to non-uniform heat current in a fire. Once this happened, a secondary disaster could be unavoidable. So, the structure safety issue of high-rise buildings has also attracted a great attention in the research field.

(4) Crowd evacuation in high-rise buildings in case of a fire becomes a major safety issue. In a fire environment, personnel evacuation behavior in high-rise buildings shows complex multi-directional characteristics. For example, in China, since elevators are prohibited in a fire, using stairs becomes the only evacuation way. However, a series of problems come as follows. How to evacuate if the only escapable stairs are blocked by smoke? How the elder and the disabled escape through the stairs? How to solve the problem of blockage caused by crowded evacuation? All these problems needed to be solved for high-rise fire, otherwise, this may lead to serious consequences.

In order to meet the above research requirements, a National Basic Research Program (973 program) of China entitled "Research on key fundamental aspects of high-rise building fire protection" has been setup by

[a] Corresponding author. Email: sunjh@ustc.edu.cn.
[b] Corresponding author. Email: hlh@ustc.edu.cn.

Ministry of Science and Technology (MOST) of China in 2012. This paper reviews the current state of art of research on fire dynamics of high-rise buildings, including the up-to-date progress of this project. The following three subjects on fire dynamics of high-rise buildings are focused in this review: the ejected flame and fire plume behavior over facade out of the window, the flame spread behavior over facade thermal insulation materials, and the buoyancy-driven smoke transportation characteristics along long vertical channels in high-rise buildings. Prospective future works are also discussed and summarized.

II. FACADE FLAME BEHAVIOR AND PLUME CHARACTERISTICS FROM WINDOW

A. Facade flame ejecting behavior and plume characteristics

The basic and classical research on facade plume characteristics was started in 1960 by Yokoi[1] by a reduced-scale model of 0.4 m × 0.4 m × 0.2 m enclosure in over-ventilated condition that no combustion outside the window. A non-dimensional parameter predicting the axis temperature for various window geometries was built up as

$$\Theta = \Delta T_Z r_0^{5/3} \left(\frac{\dot{Q}^2 T_\infty}{C_p^2 \rho_Z^2 g} \right)^{-\frac{1}{3}}, \tag{1}$$

where Θ is the temperature of the spurting gas, subscript "Z" is the distance from the window surface along the axis of the jet where the temperature rise is ΔT, r_0 is the equivalent radius of the window and defined as $r_0 = \sqrt{HB/(2\pi)}$ (B and H are width and height of the window respectively), T_∞ is the absolute atmospheric temperature, C_p and ρ are the specific heat at constant pressure and density of the spurting gas respectively, $\dot{Q}$ is the convective heat flow rate at the window, and g is the gravity acceleration. Experimental data were plotted with the non-dimensional temperature Θ versus the normalized height from the opening Z/r_0, showing three regions as similar to fire plumes (as shown in Fig. 1).

Later on, Bohm and Rasmussen[2] measured how the external flame height and radiation on the facade are affected by the rate of heat energy released outside the window. Models on ejected flame height were developed by Thomas and Law[3], Seigel,[4] and Webster et al.[5] Some large-scale[6–8] and middle-scale experiments[9,10] were carried out on heat flux exposure to facade walls. The effect of wind,[11,12] window soffit,[13] and balcony[14] on the facade plume behavior outside the window were addressed. Heskestad,[15] Klote and Milke[16] proposed entrainment correlation models for a window facade plume, and compared with that of an axisymmetric plume. Yamada et al.[17] studied the combustion efficiency and equivalence ratio, and found these two coefficients similar with the observation obtained by Gottuk et al.[18] Yamaguchi et al.[19] modified Yokoi's model

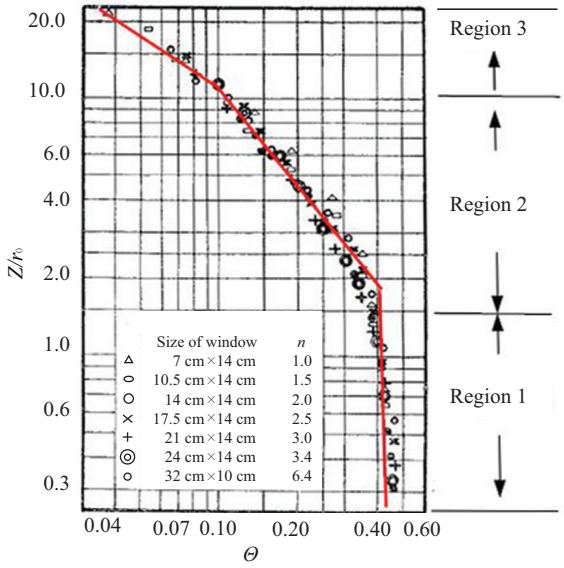

Fig. 1. Non-dimensinal temperature Θ versus the normalized height from the opening Z/r_0[1]

by applying the neutral plane concept. It was verified that the air inflow rate (kg/s) through the window of an under-ventilated enclosure fire depended on the ventilation factor brought up by Kawagoe[20] as

$$\dot{m}_a = 0.5A\sqrt{H}, \tag{2}$$

where $A(\mathrm{m}^2)$ and $H(\mathrm{m})$ are area and height of the window respectively. The heat release rate (kW) inside the enclosure for under-ventilated conditions is then expressed as

$$\dot{Q}_{\text{inside}} = \dot{m}_a \Delta H_{ox} = 3\,000 \times 0.5A\sqrt{H} = 1\,500A\sqrt{H}, \tag{3}$$

where ΔH_{ox} represents the heat released per mass of air consumed in the enclosure.

More recently, this relationship were verified by Lee et al.[21–24] through a small-scale model of 0.5 m × 0.5 m × 0.5 m fire compartment, and meanwhile a modified model on facade flame height was proposed based on characteristic length scales

$$\frac{Z_f - Z_n}{\ell_1} = f(\dot{Q}^*_{ex}) = f\left(\frac{\dot{Q}_{ex}}{\rho_\infty C_p T_\infty \sqrt{g} \ell_1^{5/2}} \right), \tag{4}$$

$$\ell_1 = (A\sqrt{H})^{2/5}, \tag{5}$$

$$\dot{Q}_{ex} = \dot{Q} - \dot{Q}_{\text{inside}}, \tag{6}$$

where Z_f is the mean (50% intermittency) flame height, Z_n is the location of the neutral plane, and ℓ_1 is the characteristic length scale. These equations depict a simple physical mechanism that flame ejecting behavior is due to the mixture of excess fuel outside the fire compartment when the heat release rate inside surpasses

the critical value. The behavior of facade flame height is found to fall into two regimes according to the non-dimensional excess heat release rate $\dot{Q}^*_{\rm ex}$, i.e., the "wall fire" regime and the "(half) axisymmetric fire" regime. Another two characteristic length scales were also defined as $\ell_2 = (AH^2)^{1/4}$ and $\ell_3 = (AH^{4/3})^{3/10}$, representing the competition of momentum to buoyancy strength, and length of flames when it turns from horizontal to vertical.

Delichatsios et al.[25] also proposed a new correlation for gas temperature inside enclosure based on energy balance. Later, Tang et al.[26] carried out reduced-scale model experiments with a 0.8 m cubic enclosure model. Their experimental data claim that the temperature inside the enclosure can be expressed as

$$\Delta T = \frac{1\,500A\sqrt{H}/A_{\rm T}}{h_{\rm c} + 0.5C_pA\sqrt{H}/A_{\rm T}}, \tag{7}$$

where $A_{\rm T}$ represents the total surface area of the enclosure, and $h_{\rm c}$ represents the overall effective heat loss coefficient.

In addition, a virtual origin model was introduced[26] in correlating the vertical temperature profile of facade fire plume

$$\Theta = 8.66\left(\frac{Z - Z_{\rm n} - Z_0}{\ell_1}\right)^{-5/3}, \tag{8}$$

where Z_0 is the location of the virtual origin, calculated by dimensionless convective heat release rate $\dot{Q}^*_{\rm conv}$ as

$$\frac{Z_0}{\ell} = 2.2(\dot{Q}^*_{\rm conv})^{2/5} - 4.14. \tag{9}$$

Hu et al.[27] also have derived a Gaussian-based mathematical model theoretically to describe the lateral temperature profile of a spill buoyant plume from window of a compartment fire as

$$\frac{\Delta T_x}{\Delta T_{\rm aw}} = \exp\left[-\beta\frac{x}{\ell_2 + \alpha\dfrac{2K+1}{2}(Z - Z_{\rm n} - Z_0)}\right], \tag{10}$$

where ΔT_x is temperature rise above the ambient, $\Delta T_{\rm aw}$ is maximum temperature rise above the ambient at adiabatic wall surface, β is Gaussian profile constant, and α is the entrainment coefficient. Meanwhile, the effective plume thickness is deduced by accounting for the entrainment rate from the non-constrained sides

$$L = \ell_2 + \alpha\left(\frac{2K+1}{2}\right)(Z - Z_{\rm n} - Z_0). \tag{11}$$

Additionally, a transitional phase where flames are ejected from the window intermittently has been found by Hu et al.[28] from the over-ventilated phrase (no flame ejected) to the full under-ventilated phrase (continuous flame ejected). A probability index is induced to describe the intermittency of flame ejection, which is ranged from 0 to 1 as a function of non-dimensional excess heat release rate as well as the ratio of heat generation to heat loss inside the enclosure in terms of $P = function(\dot{Q}^*_{\rm ex},\ \rho_\infty C_pA\sqrt{gH}/(h_{\rm c}A_{\rm T}))$.

B. Facade flame behavior and plume characteristics with external boundary wall constraints

In the last 30 years, there are also large amounts of research on the flame ejecting behavior under various external boundary wall constraint conditions induced by, for example, window eave, facing wall or side walls.

In 1990, a series of full-scale experiments were conducted with two kinds of external structures applied to the facade, i.e., a horizontal window eave, or two side walls parallel located at both sides of the window. It was concluded that the window eaves can strongly decrease the fire exposure to upper facade walls. However, the presence of side walls increases the heat flux upon the facade wall significantly. Later in 2005, Yamaguchi and Tanaka[19] carried out some experiments and found out that the facade fire plume started to derivate from the original plume axis as a result of the increase in eave widths.

Effect of side wall constraints has also been addressed[19,29–31] to show that the presence of side wall can not influence the temperature inside the enclosure and the critical heat release rate $1\,500A\sqrt{H}$ kW. Recently, Tang et al.[32] have carried out experiments on the facade flame heights with side walls based on a small-scale model of 0.4 m cubic as well as scaling analysis on the plume entrainment change due to the side walls. It was found that the side walls can restrict the entrainment from side direction so that for "(half) axisymmetric fire" the facade flame height changed with their separation distance. In contrast, for "wall fire" the entrainment mainly occurs from the front direction normal to the facade, thus the facade flame height seemed to be irrelevant to side walls. A global parameter K was then deduced to describe such difference

$$K = \frac{Z_D}{Z_0} = \begin{cases} 1, & \dot{Q}^*_{\rm ex} \leqslant 1.3, \\ \dfrac{\ell_1 + 0.4\ell_2}{\ell_1\left[1 + 0.4\left(\dfrac{\ell_2}{\ell_1} - \dfrac{\ell_2}{D}\right)\right]}, & \dot{Q}^*_{\rm ex} > 1.3. \end{cases} \tag{12}$$

Here Z_D means the flame height with side walls at separation distance of D.

The study on the effect of facing wall was conducted by Yanagisawa et al.[33] in 2008. It was found that when the distance from the facing wall to the facade decreased to a critical value, the entrainment from front direction was strongly restricted and the facade flame height was increased. Then, based on non-dimensional scaling analysis, Lee et al.[21–23] suggested the critical length to be the characteristic length scale ℓ_3 in 2009 which has also been verified by Hu et al.[34]

C. Facade flame behavior and plume characteristics in a reduced pressure atmosphere at high altitude

Previous studies are mainly carried out in default in the normal atmosphere pressure at sea level. The first study on facade flame behavior and plume characteristics at high altitude was carried out recently in 2011 in Tibet Plateau (Lhasa, China, altitude 3 650 m, air pressure 0.64 atm (1 atm = 1.01×10^5 Pa)) by Tang et al.[35,36] A serials of comparative experiments have been carried out correspondingly both in Lhasa, China and Hefei, China (altitude 50 m, air pressure 1 atm) based on a small-scale model. It has been revealed that the flame is easier to be ejected out of the window, and the vertical temperature of the plume near the facade is much higher in the reduced pressure atmosphere, and the temperature decays faster laterally (normal to the facade) in the plume, than those in the normal pressure. The air mass inflow rate (kg/s) was modified as a result of the lower air density, and the corresponding critical heat release rate (kW) was changed accordingly

$$\dot{m}_{\mathrm{a}} = 0.13\rho_\infty A g^{1/2} H^{1/2} \approx 0.35 A H^{1/2}, \tag{13}$$

$$\dot{Q}_{\mathrm{inside}} = 0.133 \frac{\Delta H_{\mathrm{ox}}}{C_p T_\infty} C_p T_\infty \rho_\infty A g^{1/2} H^{1/2} = 3\,000 \times 0.35 A H^{1/2} \approx 1\,000 A H^{1/2}, \tag{14}$$

in which ρ_∞ is the density of air.

They have also found that the entrainment strength of the facade fire plume is weaker in reduced pressure atmosphere, with the entrainment coefficient in Lhasa, China (0.64 atm) to be 0.8 times of that in Hefei, China (1 atm).

The above models and characteristic length scales have built a solid base for facade fire behavior research. Future prospective works should be done for such facade fire behaviors under more special boundary conditions, for example, with a slope constraint for hillside buildings, or with external wind flow of different directions relative to the facade.

III. FLAME SPREAD BEHAVIOR OVER FACADE THERMAL INSULATION MATERIALS OF HIGH-RISE BUILDINGS

A. Classic flame spread models over solid combustible surfaces

Flame spread behaviors over solid surfaces are the combined results of the heat and mass transfer in solid and gas phases, the pyrolysis in solid phase and the chemical reaction in gas phase. These processes result in the complexity of flame spread behaviors. In the real fire scenario, flame spread behaviors are affected by lots of factors, such as the ambient flow velocity, the oxygen concentration, the pressure, the radiation intensity, and so on. The controlling mechanisms of flame spread behavior are different in different external conditions. The flame spread models can be classified according to their features: (1) the heat transfer models and the chemical kinetic models, according to in which model the chemical kinetic reaction are considered (the chemical kinetic process can be ignored in heat transfer model, and the heat transfer process is dominant); (2) the opposed flow flame spread models and the con-current flame spread models, based on whether the direction of flame spread is the same with the ambient flow direction; (3) the horizontal flame spread models, the upward flame spread and the downward flame spread models, based on the direction of flame spread relative to the gravity direction.

The common thermal insulation materials in high-rise buildings are thermoplastic material, such as the extruded polystyrene (XPS) and the expanded polystyrene (EPS). These materials would melt, and then the melted materials drop and flow. These behaviors caused the differences of flame spread behaviors over the thermoplastic material from the common thermosetting material. Considering the flame spread behavior differences between these two kinds of materials, the classic flame spread models over solid surface are reviewed from the aspects of thermoplastic materials and the thermosetting materials.

1. Flame spread models over thermosetting materials

(1) The deRis model[37]

deRis has built still now the most basic theory on flame spread over combustible surface. Two dimensional conservation equations are solved to develop a basic understanding of the flame propagation mechanism. Figure 2 shows the "triple-flame" structure postulated by deRis, where U_{f} and U_∞ are velocities of the flame spread and the opposing flow. He has distinguished the materials as either thermally thin or thermally thick, and derived the flame spread speed model, respectively as

$$V_{\mathrm{f,thin}} = \frac{\sqrt{2}\lambda_{\mathrm{g}}}{p_{\mathrm{s}} d_{\mathrm{s}} d} \frac{T_{\mathrm{f}} - T_{\mathrm{v}}}{T_{\mathrm{v}} - T_\infty} \text{ (for thermally thin)}, \tag{15}$$

$$V_{\mathrm{f,thick}} = V_r \frac{\lambda_{\mathrm{g}} \rho_{\mathrm{g}} c_{\mathrm{g}}}{\lambda_{\mathrm{s}} \rho_{\mathrm{s}} c_{\mathrm{s}}} \cdot \frac{(T_{\mathrm{f}} - T_{\mathrm{v}})^2}{(T_{\mathrm{v}} - T_\infty)^2} \text{ (for thermally thick)}, \tag{16}$$

where ρ_{s}, c_{s}, λ_{s} are the density, specific heat, the thermal conductivity of the solid, ρ_{g}, c_{g}, λ_{g} are the density, specific heat, the thermal conductivity of the gas, T_{f}, T_{v}, T_∞ are the thermal enthalpies of flame, the fuel, the ambient, and d is the thickness of the fuel.

(2) The Quintiere model[38]

The direction of flame spread is the same with the flow direction in con-current flame spread, which is

different from the opposed flow flame spread. Flame spread model of Quintiere is a classic concurrent flame spread model.

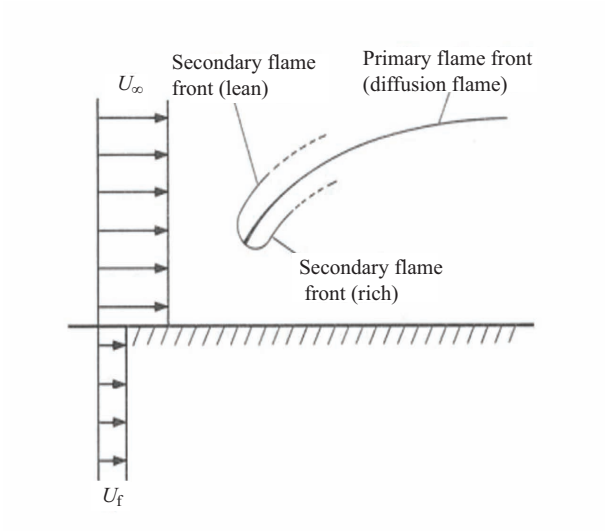

Fig. 2. The flame spread model by deRis.[37]

Figure 3 shows the illustration of concurrent flame spread over solid surface. The solid materials including three parts in flame spreading: the burned zone, the pyrolysis zone, and the preheated zone. The front of the burned zone is x_b, and the front of the pyrolysis zone is x_p. The preheated zone means the distance from the pyrolysis front to the point where its temperature is the ambient temperature, which is represented by δ_{ph}. The length of preheated zone depends on the flame length, and it usually equals to the distance from the pyrolysis front to the flame front $(x_f - x_b)$. The following concurrent flame spread model could be obtained by the energy balance analysis on the preheated zone.

$$V_f = \frac{dx_p}{dt} = \frac{x_f - x_p}{t_{ig}},$$
$$t_{ig} = \rho C_p d\left(\frac{T_p - T_s}{\dot{q}_f''}\right) \text{(for thermally thin)}, \quad (17)$$
$$t_{ig} = \frac{\pi}{4} k\rho C_p \left(\frac{T_p - T_s}{\dot{q}_f''}\right)^2 \text{(for thermally thick)},$$

where T_p is the ignition temperature, T_s is the surface temperature, $\dot{q}_f''$ q_f is the flame heat flux, k is the thermal conductivity of solid, t_{ig} is the required time for the temperature rise of solid combustible material from T_s to T_p. Usually, we supposed that the flame length x_f have the following relationship with the heat release rate per width

$$x_f - x_b = K[\dot{Q}']^n, \quad (18)$$
$$\dot{Q}' = \int_{x_b}^{x_p} \dot{Q}''(\xi)d\xi, \quad (19a)$$

where $\dot{Q}'$ and $\dot{Q}''$ are the heat release rate per unit width and per unit area. Supposing $x_b = 0$, Eq. (19a) could be rewritten as

$$\dot{Q}'(t) = x_p(0)\dot{Q}''(t) + \int_0^t \dot{Q}''(t-s)V(s)ds. \quad (19b)$$

Combining Eqs. (17), (18) and (19b), an integration model of concurrent flame spread rate over solid surface can be established.

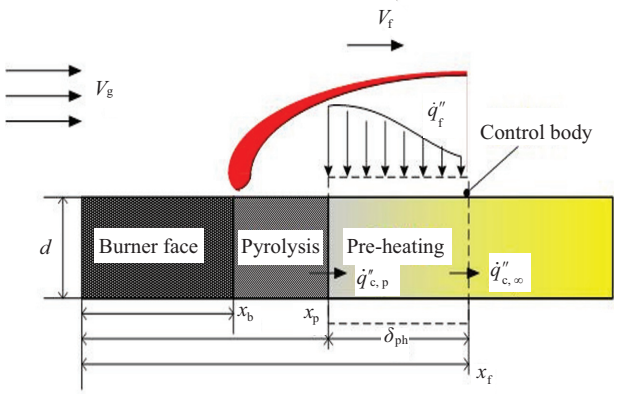

Fig. 3. Flame spread model of Quintere.[38]

2. Flame spread model over thermoplastic materials

Delichatsios[39] established a flame spread model over thermoplastic material in opposed flow. In this model, enough heat is required for the melting and pyrolysis of the material to maintain the flame spread behaviors over thermoplastic materials. The following energy conversation equation of flame spreading over thermoplastic materials is established

$$\rho_s v_f\{\delta_{v,s}[c_s(T_m - T_\infty) + L_m] + \delta_{v,l}c_l(T_p - T_m)\} = ((\dot{q}_c'')_{crit} - (\dot{m}'')_{crit}L)\delta_g, \quad (20)$$

where $\delta_{v,s}$ is the melting depth, and $\delta_{v,l}$ is the pyrolysis depth. The terms in left hand includes three parts: the heat for rising the temperature of thermoplastic material from the initial temperature to the melting temperature T_m, the melting latent heat L_m of thermoplastic materials, and the heat for rising the temperature of the melting material from the melting temperature to its pyrolysis temperature.

Then, the flame spread model over thermoplastic material can be calculated by

$$\sqrt{\frac{v_f\rho_s c_s k_s}{v_a\rho_g c_g k_g}} = \frac{(B-r)L}{c_g[L_m/c_s + (T_m - T_\infty)]} \approx \frac{T_f - T_p}{L_m/c_s + (T_p - T_\infty)}, \quad (21)$$

where v_a is the velocity of the opposed flow.

Zheng et al.[40] established a numerical model of flame spread over thermoplastic material, in which the influences of the latent heat of phase change, the heat capacity of liquid and the heat conduction are considered. Figure 4 shows the illustration of flame spread over thermoplastic materials in opposed flow.

$$\frac{v_f}{u_\infty} = \frac{\rho_g C_{pg} k_g}{\rho_l C_{pl} k_l} \left(\frac{T_f - T_i}{T_i - T_m} \right)^2 \cdot \operatorname{erf}\left(c \sqrt{\frac{1}{2} \frac{a_s}{a_l}} \right)^2, \quad (22)$$

where T_i is the flame temperature in the interface, c is the constant and usually represents the path of the interface between liquid phase and the solid phase. When c decreases to 0, T_m becomes closer to T_i. When the phase change of thermoplastic material happens, the Stephen number $St = C_{ps}(T_m - T_\infty)/L_m$ changes into the non-dimensional parameter. The Stephen number means the ratio of the heat which rising the solid temperature from the ambient to the melting temperature to the melting latent heat. When $St \to \infty$, Eq. (8) changes into the flame spread rate formula without phase change, and it also could be described by the de-Ris model. Therefore, the flame spread rate increases with the increasing of St. It is also seen that the flame spread would increase with the decrease of the specific heat C_{pl} or the heat conductivity k_l of the melting liquid.

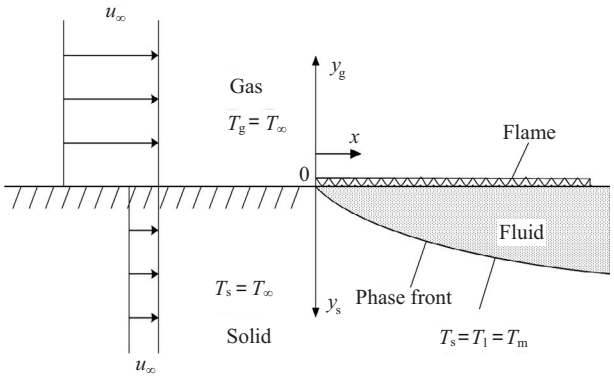

Fig. 4. Flame spread model over thermoplastic material in opposed flow by Zheng.[40]

B. Flame spread over XPS and EPS

XPS and EPS are the common thermal insulation materials in high-rise buildings, and are also the main factors causing the high-rise building fire. Guyot,[41] Levchik and Weil[42] have reviewed the research results of the pyrolysis properties of polystyrene, and Gurman et al.[43] and Paabo[44] have reviewed the research results of the toxicity of polystyrene and the polyurethane form. Kemmlein et al.[45] has showed that the smoke generation rate increase with the increasing of the bromine number in bromide flame retardant addition to the insulation material (including EPS and XPS). The fire hazards of EPS has been studied by Doroudian and Omidian[46] in which the toxic gas and the flame spread rate are deemed to be the most dangerous factors of insulation materials in fire. Cleary and Quintiere[47] have found that the melting effect and the caused radiation by pool fire would increase the flame spread rate over horizontal EPS.

Ohlemiller et al.[48] have found that, in the combustion tests over vertical EPS, the heavy smoke generated adheres to the material surface, and then prevents the further spreading and the flowing of the melting polystyrene. Griffin et al.[49] have found that the fixed method of sandwich panel plays a very important influence on the prevention of the flowing of the pyrolysis gases and the melting EPS, which can limit flame spread and the occurrence of flashover furthermore according to ISO9705 and ISO13784-1. Crescitelli et al.[50] have found that flame spread rate does not show invert ratio to the thermal diffusion coefficient when metal and inert powders were added into the polystyrene. The heat conductivity of material had an important influence on flame spread rate, that is, flame spread rate increased with the increasing of heat conductivity. Blasi and Wichman[51] have conducted experiments to test the solid-phase properties on flames spreading over composite materials.

Recently, quite a number of high-rise building fires in China occurred due to the thermal insulation materials, so the fire properties of the insulation material attracted focused attentions of the Chinese researchers.

Ji et al.[52,53] have carried out extensive combustion tests of the external wall thermal insulation system according to GB/T 8625-2005. The influence of the depth of the thermal insulation material on the flame spread behaviors are explored. Jiang[54] has studied the flame radiation properties of polystyrene fire under ventilation and found that the soot in flame and the heat release rate depends on the ventilation. Zou et al.[55] experimentally studied the flame spread behaviors over several kinds of horizontal combustibles under external radiation, and they obtain the influence of radiation intensity.

Huang et al.[56,57] have conducted extensive works on flame spread property over the thermal insulation materials. Sun et al.[56,58] explored systematically the influence of the sample size (sample depth, sample width, etc.) on flame spread over EPS and XPS. They found that flame spread rate over XPS and EPS increased with the sample depth, which is different from the behaviors over the normal thermosetting material. However, the sample width effects of EPS and XPS are similar with the normal thermosetting material, that is, the flame spread rate drops firstly and then rises with the sample width. Zhang et al.[59] pointed out that this result was caused by the different dominant regimes in

flame spreading: the convection regime and the radiation regime.

Xie et al.[60] have explored the flame spread over the thermal insulation material according to the standard of ISO9705. Xie et al.[60] studied the influence of the flowing on flame spread behaviors over the insulation materials, and they pointed out that the melting and flowing properties are important factors which affected fire development. They also found that pool fire is much easier to be formed in PS fire.

Cheng[61] and Qi[62] have measured the ratio of heat released rate and the average combustion heat of EPS and XPS in the ISO0705 experimental setup. Then they established the risk assessment model of external wall thermal insulation system considering the fire development rate and the fire intensity, and obtained the 2D risk map of flame spreading. Moreover, they compared the flame spreading risk of EPS and XPS with other thermal insulation materials under different heat flux levels. Cui[63] has studied the heat flux distribution in flame spreading over PS. Cui has found that the distribution of heat flux depends on the material density and the adherence of flame to wall. The density affects the time of melting of material, meanwhile the adherence of flame to wall affects the angle of flame upon material.

C. Flame spread over XPS and EPS under special boundary conditions

Flame spread behaviors over the thermal insulation materials depend on the material properties and also on the ambient conditions, such as the ambient pressure (or the altitude) and the surface inclination angle.

Huang et al.[64,65] have carried out experiments on flame spread behaviors over EPS and XPS with various sample depths and sample widths at high altitude in Tibet, China. It was revealed that higher pressure benefits to flame spread rate over EPS. Moreover, the increasing trend of flame spread rate with sample width become gentle, and flame spread rate over EPS is almost independent of sample depth in the normal pressure, while have an obvious increase with sample width in the reduced pressure.

Zhang et al.[66] have also carried out a series of comparison experiments of flame spread over XPS in Hefei, China (1 atm) and Lhasa, China (0.64 atm), respectively. It was revealed that the flame spread process over thermoplastic XPS underwent three stages: the pre-heated stage, the melting stage, and the pyrolysis stage. All the durations at the three stages in Lhasa, China (reduced pressure) are longer than those in Hefei, China (normal pressure), and that might be the reason of the smaller flame spread rate in Lhasa, China.

Moreover, Huang et al.[65] also explored the inclination angle effects on flame spread over EPS and XPS. Results showed that the behaviors of flame spread over EPS and XPS are obviously different from those over thermosetting materials. For example, (1) flame spread rate drops firstly and then rises with the increasing inclination angle, rather than rises monotonously; (2) especially in the case of the downward flame spread, flame spread rate increases with the increasing of inclination angle (this is attributed to the enhancement of heat transfer to the unburned zone due to the flowing down behavior of the melting EPS and XPS); (3) a second ignition is found in the flame spreading over XPS under the large inclination angle. Zhang et al.[66,67] have studied numerically flame spread behaviors over the vertical EPS and XPS surfaces, and they have found that flame spread rate follows the laws of $v_p = 1/(\alpha + \beta t)$.

The above models have well characterized the controlling mechanisms, such as chemical reaction rate, heat loss, etc., of flame spread over solid surface as well as over the thermal insulation materials under different conditions. To well understand the three-dimensional flame spread behavior along facade, how the flame spreads from outside facade into the building interior through the window with the external wind flow is needed to be quantified in the future work.

IV. BUOYANCY-DRIVEN SMOKE TRANSPORTATION BEHAVIOR IN LONG VERTICAL CHANNELS OF HIGH-RISE BUILDINGS

A. Vertical channels in high-rise buildings and special smoke transportation behaviors

High-rise buildings have extensive long vertical channel, such as stairwells, elevator shafts, cable shafts, etc. In most occasions, indoor air temperature in high-rise buildings is higher than that outdoor, which means the air density inside is lower than that outside. This density differences leads to the well-known "stack effect"[68–74] driven by buoyancy in a vertical channel. Such stack effect accelerates the smoke transportation along the vertical channel remarkably in case of a fire.[69,75] However, "reverse stack effect" will happen when indoor air temperature is lower than that of the outdoor, which may be caused by air-conditions. It is known that "stack effect" plays an important role in smoke transportation in long vertical channels, that this behavior receives focused research attention in the past. Among all shafts, smoke movement research in stairwells is most focused on. That is due to the fact that stair shafts are important channels for evacuation. In this section, the following three subjects will be addressed and reviewed: (1) smoke transportation behavior in vertical shaft, (2) smoke transportation behavior in stairwells, and (3) smoke control by pressurization in stairwell.

B. The smoke transportation behavior in vertical shaft

The research about the smoke in vertical shaft that generated by compartment fire in high-rise building began in 1980s by Marshall[75] using a 1/5 scale model as

shown in Fig. 5. The entrainment coefficient α of the fire plume in the shaft was amended to α_b denoting the entrainment coefficient at the bottom of the shaft

$$\dot{\alpha}_b = \alpha \cos\omega. \tag{23}$$

An empirical correlation about plume entrainment between HRR and temperature rise had been deducted in Ref. 75 as

$$x_s \Delta T_{cor}/\dot{Q}_{cor}^{2/3} = (0.048\dot{M}_u/\dot{M}_{cor}) - 0.071. \tag{24}$$

The linear relation between $x_s\Delta T_{cor}/\dot{Q}_{cor}^{2/3}$ and $\dot{M}_u/\dot{M}_{cor}$ has been confirmed by experiments.

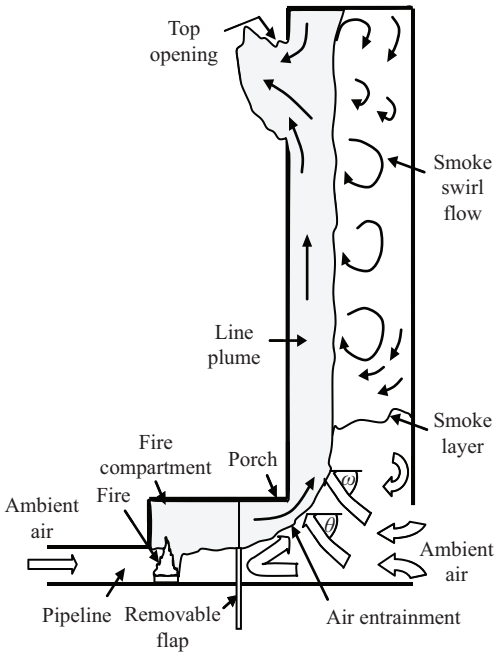

Fig. 5. Smoke flow in vertical shaft in Marshall model.[75]

In vertical shafts, two kinds of mechanisms dominates the flow pattern and hence the smoke transportation behavior.[76] One is the so-called "stack effect", and the other is turbulence mixing mechanism which is a mixing process between hot gases and air, relating to Rayleigh–Taylor mixing.[77] A simplified model of stack effect was illustrated by Harmathy[78] in 1998. An equation calculating air pressure difference between the air inside and outside the building was deduced as

$$P_a - P_s = \frac{1}{2}\rho_a^0 T_0 \left(\frac{u_w^2}{\sqrt{T_a T_i}} + \frac{u_s^2}{T_i}\right), \tag{25}$$

where T_i is the air temperature inside the building, T_a is the temperature of the external air, u_w is the air velocity that leaks from the building wall, and u_s is the air velocity that leaks through the shaft wall.

Klote and Fothengill[79] deduced equations to calculate neutral plane location in vertical shaft in different opening circumstances (including continuous opening in lateral wall, top and bottom opening in lateral wall, top opening and bottom opening), and explored a calculation procedure STACK. In a vertical shaft, ambient cold air flows into the shaft through the opening below the neutral plane and hot smoke flows out of the shaft through the openings above the neutral plane.

The amount of the hot smoke that flows out is

$$m_{out} = \frac{2}{3}K_0 C W (H_c - H_n)^{3/2} \cdot \sqrt{2\rho_c g K_p(\rho_\infty - \rho_c)}, \tag{26}$$

where H_c is the height of the shaft, H_n is the height of the neutral plane of the window. The amount of the cold gas that flows into the shaft is

$$m_{in} = \frac{2}{3}K_0 C W H_n^{3/2}\sqrt{2\rho_\infty g K_p(\rho_\infty - \rho_c)}. \tag{27}$$

When the flows are stable, the air amount flowing in equals the air amount flowing out, and combining the ideal gas equation, the position of the neutral plane can then be calculated as

$$\frac{H_n}{H_c} = \frac{1}{1 + (T_c/T_\infty)^{1/3}}. \tag{28}$$

In real fire, the uniform temperature distribution assumption in the shaft is not applicable because the temperature near the fire source is much higher than other areas. Based on Klote model,[79] the modified neutral plane position is

$$(H_c - H_n)^{3/2} = (H_f)^{3/2}(T_c/T_f)\sqrt{(T_f - T_\infty)/(T_c - T_\infty)} + (H_n - H_f)^{3/2}\sqrt{T_c/T_\infty}. \tag{29}$$

As for the turbulence mixing mechanism, Zukoski[80] employed the concept of transient local turbulence mixing rate and the Boussinesq approximation (assuming the smoke density of the upstream is approximately the air density in diffusive equation), and established the relation of turbulence diffusive rate as

$$\ell_t \propto d^2 \left(\frac{L}{d}\right)^{1/4} \sqrt{\frac{1}{\rho_\infty}\left(\frac{\partial\rho}{\partial Z}\right) g}, \tag{30}$$

where d is tube diameter. Through deduction, there is a linear relation between the normalized time and the ratio which equals the square root of the initial temperature in the shaft with the square root of transient temperature difference $\sqrt{\rho_\infty - \rho_{ini}}/\sqrt{\rho_\infty - \rho}$, and this linear relation has been confirmed by experiments.[80,81]

Chow and Fong[82] established the dimensionless model of the rising velocity of smoke front in vertical shaft. The dimensionless velocity is

$$V = \frac{v}{\sqrt{gD}} \propto \left(\frac{\dot{Q}}{C_p \rho_\infty T_\infty \sqrt{gD}}\right)^{1/3} \left(\frac{DZ}{A}\right)^{1/3}$$

$$= \dot{Q}^{*1/3} \left(\frac{DZ}{A} \right)^{1/3}. \tag{31}$$

The dimensionless time is

$$\tau = \left(t \sqrt{\frac{g}{D}} \right) \dot{Q}^{*1/3}, \tag{32}$$

where D is a characteristic size taken as the cross-section length in this case, and $\dot{Q}^*$ is the dimensionless fire heat release rate. In the equations, it was assumed that the density variations through the smoke in the shaft to the ambient air were small, i.e., $\rho \approx \rho_\infty$.
(1) When fire source located at the bottom of the shaft,

$$\tau = 8.66 Z^{2/3}. \tag{33}$$

(2) When fire source located in the adjacent room of the bottom of the shaft,

$$\tau = \begin{cases} 7.9 Z^{2/3}, & Z > 2.5, \\ 4.3 Z^{7/6}, & Z \leqslant 2.5. \end{cases} \tag{34}$$

The significant assumption that $\rho \approx \rho_\infty$ applied in Chow's model would bring large error in practical smoke flow in vertical shaft, especially when the shaft is relatively high. By employing the virtual origin concept in Heskestad plume model and virtual origin method in Harrison spill plume model, Sun[68] further developed the plume characteristics model especially for the "plume entrance region" near fire source in vertical shaft as shown in Fig. 6. A one-dimensional model is built by temperature ΔT, dimensionless temperature $\Theta(Z)$, density $\rho(Z)$, dimensionless density ϕ, velocity v, plume front z_f as

$$\begin{cases} \Delta T = T - T_0 = (T_\mathrm{i} - T_0) \mathrm{e}^{-\beta Z/H}, \\ \Theta(Z) = \dfrac{T_\mathrm{i} - T_0}{T_0} \mathrm{e}^{-\beta Z}, \\ \rho(Z) = \dfrac{p_0/R^*}{(T_\mathrm{i} - T_0)\mathrm{e}^{-\beta Z} + T_0}, \\ \phi = 1 - \dfrac{T_0}{(T_\mathrm{i} - T_0)\mathrm{e}^{-\beta Z} + T_0}, \\ v = \dfrac{R^* \dot{m}}{A p_0} [(T_\mathrm{i} - T_0)\mathrm{e}^{-\beta Z} + T_0], \\ z_\mathrm{f} = \dfrac{C_4 t^{2/3} + C_5 t^2}{C_3} \ln \left(\dfrac{T_\mathrm{i}}{T_0} \cdot \mathrm{e}^{C_2 t} - \dfrac{T_\mathrm{i} - T_0}{T_0} \right), \end{cases} \tag{35}$$

where $C_2 = \dfrac{\rho_0 h}{4DC_p}$, $C_3 = \dfrac{Ah}{4DC_p}$, $C_4 = 0.071\alpha^{2/3}$, $C_5 = 1.92 \times 10^{-3} \cdot \alpha^2$, $\beta = \dfrac{h}{C_p} \dfrac{A}{\dot{m}} \dfrac{H}{4D} = \dfrac{4hH}{4DC_p} \dfrac{1}{\dot{m}}$.

The factor β is related to initial conditions and the size of the vertical shaft and can be calculated by analysis of the fire source. During the rising process, this parameter varies with time, i.e., plume temperature, density, and rising velocity are all functions of time. In one-dimensional steady smoke motion model, the expressions of the smoke parameters are similar to those in smoke rising model. However, during the steady progress, the parameter β is only related to the initial conditions and the size of the vertical shaft while do not change with time.

C. Smoke transportation behavior in stairwells

Ergin-Ozkan et al.[83] performed the earliest studies on the formation of interface between the hot and cold air above the inclined stair. Reynolds et al.[77,84] further analyzed the mechanism of thermal buoyancy-driven air flow and proposed dimensionless relations

$$FrRe^{1/3} \propto St^{1/3}, \tag{36}$$

$$\Delta T/T \propto Re^{1/3} St^{2/3}, \tag{37}$$

in which Fr is Froude number, Re is Reynolds number, and St is Stanton number.

Marshall[85] carried out an experiment on the behavior of hot gases flowing in a 1/5 scale model of five-story staircase. It was observed that the incoming gases from the room swirl in the stairwell affected by the staircase and mix with air all the way to go up. A large amount of smoke mixes with abundant entrainment air in the inclined overflow section between burning room and stairwell. There is no distinct gas layer interface in stairwell compared with that in shafts with no blocks. Marshall's model is sufficiently enough to explain the smoke movement and the entrainment of air with door openings in the ground and top floors, however, it did not account heat transfer between hot gases with stairwell wall.

Qin et al.[73,74] have discussed the effect of different heat release rates on entrainment of air, average oxygen concentration, average temperature in stairwell, as well as maximum differential pressure in and out of stairwell using large eddy simulation (LES). Peppes et al.[76] performed experiments and simulations on mass and energy transfer processes induced by temperature differences in a three-story stairwell and discovered that flow velocity is steady in the horizontal opening within stairwell between floors. Quantitative analysis demonstrates that the flow velocity is proportional to $(\Delta T/T)^{0.3}$.

More recently, Ji et al.[86] have carried out experiments on one-third scale model showing that smoke rise time of open stairwell and closed stairwell is respectively proportional to 1.227 power and 2.135 power of non-dimensionless rise time, and both inverses proportional to 1/3 power of source power (as shown in Fig. 7).

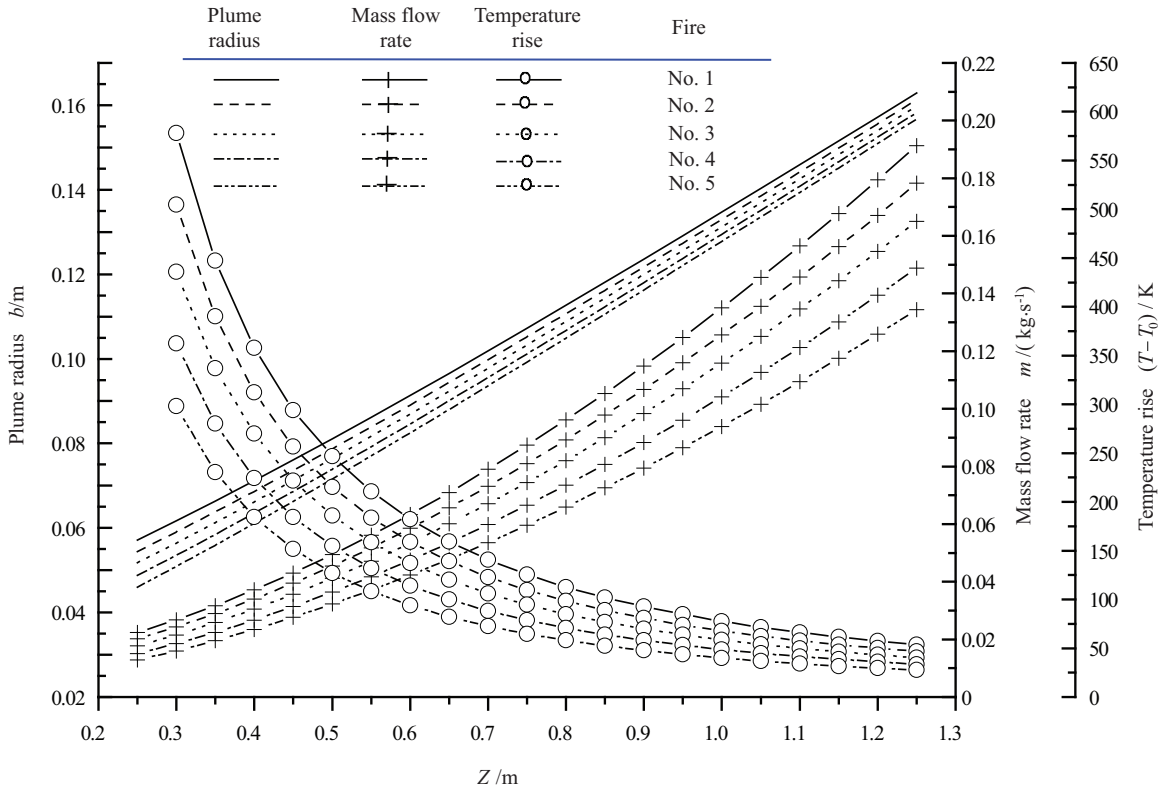

Fig. 6. Plume parameter profiles in "plume entrance region" of the source in vertical shaft change with plume height Z.[68]

D. Smoke control by pressurization in stairwell

Pressurization technique by air supply is widely used in stairwells of high-rise buildings, as to produce pressure difference between the stairwell and the fire space to prevent smoke from spreading into the stairwell. To fulfill that goal, the pressure in stairs must be higher than that in front chambers, and the pressure in front chambers must be higher than that in aisles.

Klote and Fothergill[79] carried out theoretical derivation about pressurization requirements in 1983. The relation of ΔP_{SB} (pressure difference between the stairwell and the building) versus ΔP_{SO} (pressure difference between the stairwell and outside) is

$$\Delta P_{\mathrm{SB}} = \Delta P_{\mathrm{SBb}} + \frac{3\ 460(1/T_{\mathrm{O}} - 1/T_{\mathrm{S}})Z}{1 + (A_{\mathrm{SB}}/A_{\mathrm{BO}})^2}, \tag{38}$$

$$\Delta P_{\mathrm{SB}} = \frac{\Delta P_{\mathrm{SO}}}{1 + (A_{\mathrm{SB}}/A_{\mathrm{BO}})^2}. \tag{39}$$

The air flow rate from the stairwell to the building is then calculated by

$$Q_{\mathrm{SB}} = K_{\mathrm{q}} \frac{N A_{\mathrm{SB}}}{\sqrt{\rho}} \left(\frac{\Delta P_{\mathrm{SBt}}^{3/2} - \Delta P_{\mathrm{SBb}}^{3/2}}{\Delta P_{\mathrm{SBt}} - \Delta P_{\mathrm{SBb}}} \right), \tag{40}$$

where ΔP_{SBt} is the pressure difference between the stairwell and the building, ΔP_{SBb} is pressure difference between the bottom part of the stair and the building, and K_{q}=0.613 is a constant coefficient.

Further, Evans and Klote[87] state that total air flow into the stairwell equals to the total amount leakage from the stairwell into the building and that to the outside of the building. A temperature influence factor is introduced as

$$B = 3\ 460 \left(\frac{1}{T_{\mathrm{O}} + 273} - \frac{1}{T_{\mathrm{B}} + 273} \right), \tag{41}$$

where T_{B} and T_{O} are respectively the indoor temperature and outdoor air temperature. Then the pressure difference between the stairwell and outside is

$$\Delta P_{\mathrm{SO}} = \Delta P_{\mathrm{b}} \left[1 + (A_{\mathrm{SB}}/A_{\mathrm{BO}})^2 \right] + B H_{\mathrm{bd}}, \tag{42}$$

where H_{bd} is the height from the bottom of the stairwell to the center line of door facing outside.

More recently, Sun et al.[68] discussed and analyzed systematically the effect of other factors, such as installation positions of fan, air supply volumes, fire source positions, floors with open door, and widths of the crack of the first and second door, etc., on the pressurization

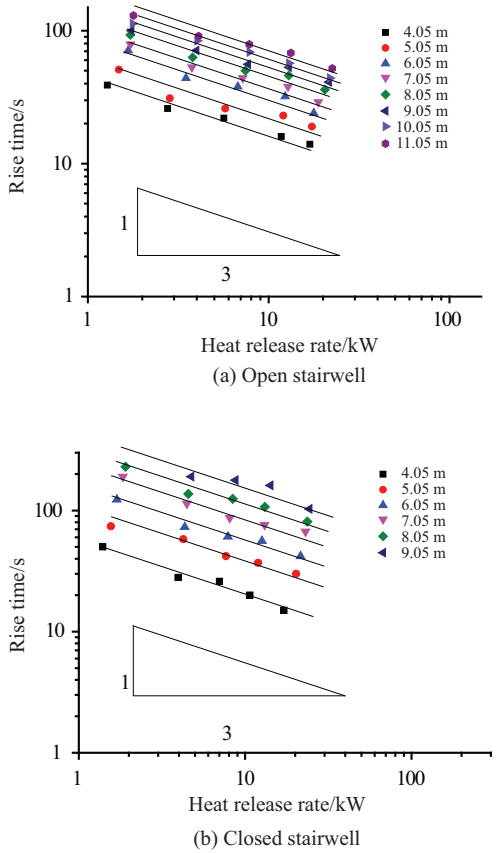

Fig. 7. Smoke rise time versus fire source power (heat release rate).[83]

performance. It revealed the following facts. (1) When the width of the crack of the first and second door is small, the pressure in the stairwell does not change a lot, and maintains at relative high value. However, when the width increases to 6 cm, the pressure decrease obviously and a critical crack width is suggested as between 4 cm and 6 cm. (2) With the increase in the volume of pressurization air, the pressure in the stairwell arises apparently, and the steady positive pressure above the fire floor increases linearly with the pressurization air volume. (3) The pressurization opening is better to be installed at the top than at the below positions of the stairwell.

The above models have well characterized the smoke transportation behavior inside the high-rise buildings through long vertical channels. Under the special three-dimensional smoke transportation (inside-outside-inside), it remains to be answered and quantified that how the flow condition inside the building is affected by the external wind flow once the window is broken by the fire, and how the outside facade fire smoke is pushed back into the building through the wind by the external wind flow remain to be answered and quantified.

V. CONCLUDING REMARKS

Fire safety of high-rise building has attracted extensive attention and focus due to serious fire accidents recently in China. This paper reviews the current state of art of research on fire dynamics of high-rise buildings addressing the following three important subjects: (1) the ejected flame and fire plume behavior over facade out of the compartment window, (2) the flame spread behavior over facade thermal insulation materials, and (3) the buoyancy-driven smoke transportation characteristics along long vertical channels in high-rise buildings.

The current models can well characterize the above separate processes in the three-dimensional fire spread behavior of high-rise buildings. However, to understand the whole process of this three-dimensional fire spread behavior, additional mechanisms connecting these separate processes need to be quantified in the future. For example, how the flame and smoke of the outside facade fire can spread into the building with external wind flow? And how the combustion, flow dynamics and smoke transportation behavior are affected by the external wind flow when the wind is broken by the fire? All of these important issues are ongoing research works in the 973 program Research on key fundamental aspects of high-rise building fire protection. A special issue including the most up-to-data research progress of this 973 program on thermal insulation material ignition by firebrands, structure fire safety and human crowd evacuation behavior will be reported in the future.

This work was supported by National Basic Research Program of China (2012CB719702).

1. S. Yokoi, *Study on the prevention of fire-spread caused by hot upward current*, Report 34, Report of the Building Research Institute, Japanese Ministry of Construction (1960).
2. B. Bohm and B. M. Rasmussen, Fire Safety J. **12**, 103 (1987).
3. P. H. Thomas and M. Law, Fire Prevention Sci. Techno. **10**, 19 (1972).
4. L. G. Seigel, Fire Techno. **5**, 43 (1969).
5. C. T. Webster, M. M. Raftery, and P. G. Smith, Fire Research Note 474, Joint Fire Research Organization (1961).
6. Y. W. Hui, Build. Environ **44**, 1215 (2009).
7. I. Oleszkiewicz, Fire Techno. **26**, 357 (1990).
8. Draft British Standard, Document No. 01/540504 DC, British Standards Institute (2001).
9. Uniform Building Code Standard 26-9, Test Standard of the International Conference of Building Officials **3**, 507 (1985).
10. NFPA 285, *Standard fire test method for evaluation of fire propagation characteristics of exterior non-load-bearing wall assemblies containing combustible components*, National Fire Protection Associate (1998).
11. O. Sugawa and W. Takahashi, Flow behavior of ejected fire plume from an opening with and without external wind. Proceedings of Asia flame '95, 409 (1995).
12. O. Sugawa, D. Momita, and W. Takahashi, Fire Safety Sci. **5**, 249 (1996).
13. Y. Ohmiya, S. Yusa, K. Matsuyama, et al., *Prediction method of opening jet plume behavior in the presence of an opening soffit*. Proceedings of the 5th AOSFST, 171 (2001).

14. T. Yamada, K. Takanashi, E. Yanai, et al., Fire Safety Science **7**, 903 (2003).
15. G. Heskestad, Fire Safety J. **7**, 25 (1984).
16. J. H. Klote and J. A. Milke, *Design of smoke management systems*, ASHRAE Publication 90022 (1992).
17. T. Yamada, K. Takanashi, E. Yanai, et al., *Ignition and flame spread over wire hardness in sub-atmospheric pressure*, Proceedings of the 9th International Symposium on Fire Safety Science, 903 (2003).
18. D. T. Gottuk, R. J. Roby, and C. L. Beyler, *A study of carbon monoxide and smoke yields from compartment fires with external burning*, Twenty-Fourth Symposium (International) on Combustion, Pittsburg (1993).
19. J. I. Yamaguchi and T. Tanaka, Fire Sci. Techno. **24**, 17 (2005).
20. K. Kawagoe, BRI Research Paper, No. 29, Building Research Institute (1967).
21. Y. P. Lee, *Heat fluxes and flame heights in external facade fires* [Ph.D. Thesis], University of Ulster, UK (2006).
22. Y. P. Lee, M. A. Delichatsios, and G. W. H. Silcock, Proc. Combust. Inst. **31**, 2521 (2007).
23. Y. P. Lee, M. A. Delichatsios, Y. Ohmiya, et al., Proc. Combust. Inst. **31**, 2551 (2009).
24. Y. P. Lee, M. A. Delichatsios, and Y. Ohmiya, *The study for the physics of the outflow from the opening of a burning enclosure*, Proc. 5th Inter. Semi. Fire Explos. Hazards, 381 (2007).
25. M. A. Delichatsios, Y. P. Lee, and P. Tofilo, Fire Safety J. **44**, 1003 (2009).
26. F. Tang, L. H. Hu, M. A. Delichatsios, et al., Inter. J. Heat Mass Transfer **55**, 93 (2012).
27. L. H. Hu, F. Tang, M. A. Delichatsios, et al., Inter. J. Heat Mass Transfer **56**, 447 (2013).
28. L. H. Hu, K. H. Lu, M. Delichatsios, et al., Combust. Flame **159**, 1178 (2012).
29. T. Nakao, A. Yanagisawa, A. Jo, et al., Fire Sci. Techno. **26**, 497 (2007).
30. A. Yanagisawa, A. Jo, T. Nakao, et al., Fire Sci. Techno. **26**, 505 (2007).
31. A. Jo, T. Nakao, A. Yanagisawa, et al., Fire Sci. Techno. **26**, 511 (2007).
32. F. Tang, L. H. Hu, W. Zhu, et al., J. Combust. Sci. Techno. **17**, 262 (2011).
33. A. Yanagisawa, D. Goto, Y. Ohmiya, et al., Fire Safety Sci. **9**, 801 (2009).
34. L. H. Hu, F. Tang, M. A. Delichatsios, et al., Inter. J. Heat Mass Transfer **56**, 119 (2013)
35. F. Tang, L. H. Hu, Q. Wang, et al., Inter. J. Heat Mass Transfer **55**, 5642 (2012)
36. L. H. Hu, F. Tang, D. Yang, et al., Inter. J. Heat Mass Transfer **53**, 2844 (2010).
37. J. N. deRis, *The spread of a diffusion flame over a combustible surface* [Ph.D. Thesis], Harvard University, Cambridge (1968).
38. J. Quintiere, *The Atrium, Southern Gate* (John Wiley & Sons, Chichester, 2006).
39. M. A. Delichatsios, Combustion and Flame **135**, 441 (2003)
40. G. Zheng, I. S. Wichman, and A. Benard, Combustion and Flame **124**, 387 (2001).
41. A. Guyot, Polymer Degradation and Stability **15**, 219 (1986)
42. S. V. Levchik and E. D. Weil, Polymer International **53**, 1585 (2004).
43. J. L. Gurman, L. Baier, and C. Barbara, Fire and Materials **11**, 109 (1987).
44. M. Paabo, Fire and Materials **11**, 1 (1987).
45. S. Kemmlein, O. Hahn, and O. Jann, Atmospheric Environment **37**, 5485 (2003).
46. S. Doroudian and H. Omidian, Building and Environment **45**, 647 (2010).
47. T. G. Cleary, J. G. Quintiere, NISTIR 4664 (1991).
48. T. J. Ohlemiller, J. Bellan, and F. Rogers, Combust. Flame **36**, 197(1979).
49. G. J. Griffin, A. D. Bicknell, and G. P. Bradbury, Journal of Fire Sciences **24**, 275 (2006).
50. S. Crescitelli, F. Pota, and G. Santo, Combustion Science and Technology **27**, 75 (1981).
51. C. D. Blasi and I. S. Wichman, Combustion and Flame **102**, 229 (1995).
52. G. Q. Ji, C. L. Zhu, C. Y. Song, et al., Building Science (in Chinese) **24**, 43 (2008).
53. G. Q. Ji, C. L. Zhu, C. Y. Song, et al., Building Science (in Chinese) **24**, 49 (2008).
54. F. H. Jiang, Fire Safety Journal **30**, 383 (1998).
55. Y. H. Zou, J. J. Zhou, Z. R. Zhong, et al., Journal of University of Science and Technology of China **31**, 465 (2001).
56. X. J. Huang, Y. Zhang, J. Ji, et al., Combustion Science and Technology **17**, 527 (2011).
57. X. J. Huang, *Different external environment typical insulation materials PS fire spread characteristics laws* [Ph.D. Thesis], University of Science and Technology of China, Hefei (2011).
58. Y. Zhang, J. H. Sun, and X. Huang, International Journal of Heat and Mass Transfer **61**, 28 (2013).
59. Y. Zhang, X. Huang, and Q. Wang, Journal of Hazardous Materials **189**, 34 (2011).
60. Q. Xie, H. Zhang, and R. Ye, Journal of Hazardous Materials **166**, 1321 (2009).
61. X. D. Cheng, *Combustion behavior and melt flow of typical thermoplastic material in confined spaces* [Ph.D. Thesis], University of Science and Technology of China, Hefei (2010).
62. Y. J. Qi, *Fire characteristics of common organic EIFS* [Ph.D. Thesis], University of Science and Technology of China, Hefei (2012).
63. Y. Cui, *Common organic wall insulation fire behavior under vertical wall conditions* [Ph.D. Thesis], University of Science and Technology of China, Hefei (2012).
64. X. J. Huang, Q. S. Wang, Y. Zhang , et al., Journal of Thermoplastic Composite Materials **25**, 427 (2012).
65. X. J. Huang, J. H. Sun, J. Ji, et al., Chinese Science Bulletin **56**, 1617 (2011).
66. W. Zhang, G. Q. Zhu, and L. Zhang, Journal of Safety Science and Technology **8**, 11 (2012).
67. Y. F. Xie, G. Q. Zhu, and L. Zhang, Journal of Safety Science and Technology **3**, 28 (2012).
68. X. Q. Sun, *Smoke flow and control research in vertical high-rise building channel* [Ph.D. Thesis], University of Science and Technology of China, Hefei (2009).
69. X. Q. Sun, L. H. Hu, W. K. Chow, et al., International Journal of Heat and Mass Transfer **54**, 910 (2011).
70. X. Q. Sun, L. H. Hu, Y. Z. Li, et al., Applied Thermal Engineering **29**, 2757 (2009).
71. S. B. Riffat, J. Walker, and J. Litter, *Zone to zone tracer gas measurements laboratory calibration and values of air flows up and down stairs in houses*, Proceedings of the 9th ATVC Conference, 85 (1988).
72. R. Edwards and C. Irwin, *Two-directional air movements in stairwells*, Proceedings of the 11th ATVC Conference **21**, 379 (1990).
73. T. X. Qin, Y. C. Guo, C. K. Chan, et al., Building and Environment **40**, 183 (2005).
74. T. X. Qin, Y. C. Guo, C. K. Chan, et al., Journal of Engineering Thermophysics **25**, 177 (2004).
75. N. R. Marshall, *Air Entrainment into Smoke and Hot Gases in Open Shafts* (Fire Research Station, Borehamwood, 1984).
76. A. A. Peppes, M. Santamouris, and D. N. Asimakopoulos, Building and Environment **37**, 497 (2002).
77. A. J. Reynolds, M. R. Mokhtarzadeh-Dehghan, and A. S. Zohrabian, Building and Environment **23**, 63 (1980).

78. T. Z. Harmathy, Fire Technology **34**, 6 (1998).
79. J. H. Klote and J. W. Fothergill, U.S. Dept. of Commerce, National Bureau of Standards ASHRAE (1983).
80. E. E. Zukoski, *A review of flows driven by natural convection in adiabatic shafts*, NIST-GCR-95-679 (1995).
81. J. B. Cannon and E. E. Zukoski, Technical Fire Report No. 1 to the National Science Foundation, California Institute of Technology, Pasadena (1975).
82. W. K. Chow and N. K. Fong, *The PolyU/USTC Atrium: A full-scale burning facility for atrium fire studies*, Proceeding of the First International Symposium on Engineering Performance-Based Fire Codes, Hong Kong, 186 (1998).
83. S. Ergin-Ozkan, M. R. Mokhtarzadeh-Dehghan, and A. J. Reynolds, International Journal of Heat and Mass Transfer **38**, 2159 (1995).
84. A. J. Reynolds, Building and Environment **21**, 149 (1986).
85. N. R. Marshall, Fire Safety Journal **9**, 245 (1985).
86. J. Ji, L.J. Li, W.X. Shi, et al., J. Heat Mass Transfer **64**, 193 (2013).
87. D. H. Evans and J. H. Klote, Smoke control provisions of the 2000 IBC: An interpretation and application guide, International Conference of Building Officials (ICBO), 1 (2003).